

See discussions, stats, and author profiles for this publication at: <https://www.researchgate.net/publication/230821370>

# Biomass Oxidative Flash Pyrolysis: Autothermal Operation, Yields and Product Properties

ARTICLE in ENERGY & FUELS · FEBRUARY 2012

Impact Factor: 2.79 · DOI: 10.1021/ef201662x

CITATIONS

43

READS

75

5 AUTHORS, INCLUDING:



**Maider Amutio**

Universidad del País Vasco / Euskal Herriko U...

46 PUBLICATIONS 782 CITATIONS

SEE PROFILE



**Gartzen Lopez**

Universidad del País Vasco / Euskal Herriko U...

81 PUBLICATIONS 1,453 CITATIONS

SEE PROFILE



**Roberto Aguado**

Universidad del País Vasco / Euskal Herriko U...

68 PUBLICATIONS 1,997 CITATIONS

SEE PROFILE



**Martin Olazar**

Universidad del País Vasco / Euskal Herriko U...

274 PUBLICATIONS 5,688 CITATIONS

SEE PROFILE

# Biomass Oxidative Flash Pyrolysis: Autothermal Operation, Yields and Product Properties

Maider Amutio, Gartzzen Lopez, Roberto Aguado, Javier Bilbao, and Martin Olazar\*

Department of Chemical Engineering, University of the Basque Country UPV/EHU, P.O. Box 644-E48080 Bilbao, Spain

**ABSTRACT:** Biomass autothermal flash pyrolysis has been carried out by adding oxygen to the reaction environment in a bench-scale plant provided with a conical spouted bed reactor, at 500 °C and using two oxygen concentrations in the inlet gas stream (2.5 and 4.1 vol %, which correspond to equivalence ratios of 15 and 25, respectively). An increase in the oxygen concentration leads to an increase in gas and water yields, whereas there is a decrease in the yield of both char (partially burned) and organic compounds in the bio-oil, albeit only slightly in the latter case. Bio-oil composition undergoes only minor changes for certain individual components. The experimental results highlight the advantages of the conical spouted bed reactor (CSBR) for scaling up the autothermal operation. A study on energy requirements reveals that the oxygen concentration needed to achieve autothermal operation decreases as the scale is larger. The oxygen content required in the inlet gas stream for autothermal operation in an industrial-scale plant of 500 kg h<sup>-1</sup> is 2.7 vol %, and neither bio-oil yield nor composition is significantly affected, being similar to the case of operating in an inert atmosphere.

## 1. INTRODUCTION

There is a growing interest in the research into alternative raw materials to petroleum, with the aim being to find a solution to the depletion of petroleum reserves and to the increasing demand for energy, automotive fuels, raw materials for today's petrochemical industry, and H<sub>2</sub>, as well as tackling the environmental problems associated with fossil fuels. Biomass is regarded as the most promising alternative to fossil fuels, given that if it is properly exploited it does not contribute to a net rise in the level of CO<sub>2</sub> in the atmosphere. Furthermore, it is the only renewable source of fixed carbon that can be converted into liquid, solid, and gaseous fuels and used for generating both heat and power.

The biorefinery concept has been widely developed, basically involving the sustainable valorization of biomass to obtain transportation fuels and valuable chemicals by subjecting the biomass to several processes, such as gasification, pyrolysis, or hydrolysis.<sup>1–3</sup> Pyrolysis is one of the technologies with the best industrial perspectives, because the process conditions can be optimized to maximize the yields of gas, liquid, or char, which can be treated separately.<sup>4,5</sup> Furthermore, the production of the liquid fraction, or bio-oil, by means of lignocellulosic biomass flash pyrolysis can be carried out in rural areas and at a moderate scale (in mobile units). The bio-oil can be transported to upgrading plants: either to refinery units, where adequate acid catalysts can selectively convert it into olefins<sup>6</sup> or aromatics,<sup>7</sup> or to large power plants to convert it into heat and power. Furthermore, the bio-oil can also generate H<sub>2</sub> using a bifunctional reforming catalyst<sup>8</sup> and can be cofed into refinery units, where the processes attracting more attention are FCC (fluid catalytic cracking) units<sup>9</sup> and the MTO (methanol to olefins) process.<sup>10</sup>

Biomass flash pyrolysis is carried out at moderate temperatures (around 500 °C), with high heating rates (10<sup>3</sup>–10<sup>4</sup> K s<sup>-1</sup>), short vapor residence times (typically below 1 s), rapid removal of the char from the reaction environment, and rapid cooling of the pyrolysis vapors. These characteristics maximize bio-oil yield,

given that secondary cracking reactions are minimized, and a bio-oil yield typically in the 60–80 wt % range is obtained, with a gas yield in the 10–20 wt % range and a char yield in the 15–25 wt % range.<sup>5,11,12</sup> Gas and char byproducts can be used to supply energy to the pyrolysis process or, in the case of char, for the production of active carbon for purification processes and for metallic or acid catalyst support.<sup>13–15</sup> Furthermore, its potential for soil amendment can also be exploited.<sup>16</sup>

A wide range of reactor configurations has been used for biomass flash pyrolysis, with the more outstanding ones being fluidized bed reactors,<sup>17–19</sup> transport and circulating fluidized bed reactors,<sup>20–22</sup> ablative reactors (rotating and cyclonic),<sup>23</sup> auger reactors,<sup>24</sup> vacuum reactors,<sup>25</sup> and conical spouted bed reactors.<sup>26,27</sup> Several configurations have been scaled up to demonstration or commercial plants, especially fluidized bed reactors, such as the Dynamotive process (8000 kg h<sup>-1</sup>) and the Ensyn transported bed reactor (4000 kg h<sup>-1</sup>), both located in Canada. However, some such plants have been dismantled or are not competitive because of the high cost compared to fossil-based energy production.<sup>5</sup>

The conical spouted bed reactor (CSBR), which is an alternative to fluidized beds, performs well for biomass flash pyrolysis.<sup>26,27</sup> The vigorous cyclic particle movement allows handling particles of irregular texture, fine particles, sticky solids, and those with a wide size distribution, with no agglomeration problems,<sup>28,29</sup> contributing to a high heating rate and high heat and mass transfer rates between phases.<sup>30,31</sup> Additionally, the great versatility of the gas flow rate allows operating with short gas residence times (as low as milliseconds) in the dilute spouted bed regime.<sup>32</sup> Consequently, the bio-oil yields obtained with this reactor are very high in a wide range of temperatures, from 71 wt % at 400 °C to 75 wt % at 500 °C,<sup>27</sup> with these values being close

Received: October 26, 2011

Revised: December 30, 2011

Published: January 9, 2012



to the maximum obtainable yield predicted by the macrokinetic model of Calonaci et al.<sup>33</sup> In addition, several improvements have been carried out in previous studies for scaling up the process, which are additional advantages to the CSBR's simplicity and low building cost. First, the hydrodynamic problems involved in scaling up the reactor are solved by the use of internal devices that improve bed stability and reduce gas flow rate requirements.<sup>34</sup> Second, the conical spouted bed technology allows continuous operation, as char is continuously removed from the reactor.<sup>27</sup> Finally, vacuum operation reduces the gas flow rate to be heated to the reaction temperature and simplifies bio-oil condensation, reducing the associated costs.<sup>35</sup> Furthermore, the excellent performance of the conical spouted bed reactor has been confirmed in the scaling up of the biomass pyrolysis process, with the development of a 25 kg h<sup>-1</sup> pilot plant.<sup>31</sup>

One of the greatest challenges when scaling up the pyrolysis process is the heat supply to the reactor, specifically the energy required to heat the raw material to the process temperature.<sup>5</sup> There are several heat-supply strategies depending on the reactor configuration (with most of them having several limitations): (i) heating through the reactor walls, with the ratio between the wall area and the mass contained in the bed being generally very low, and consequently, the heat transfer rate is also low; (ii) heating through internal heating devices, which affect the hydrodynamics of the process, increase the complexity of the design, and experience rapid fouling as a result of the tar and soot present in the bed during the pyrolysis process; (iii) heating through fluidizing gas, although heat can be supplied only partially because of certain limitations, such as gas bypassing the reactor (leading to local overheating or underheating) and the limited flexibility of the inlet gas flow rate and temperature; (iv) removing and heating the bed material in a separate reactor, which although it increases the complexity of the system, is used in most transported and circulating fluidized bed reactors, where the heat required is supplied by char combustion,<sup>36</sup> and (v) the addition of small amounts of oxygen to the pyrolysis reactor, which do not significantly affect the process, although local overheating may occur.

In this study, oxidative pyrolysis is proposed as a simple and economical way to improve process adaptation to industrial scale, given that the energy required for the process is supplied in the pyrolysis reaction itself by the combustion of part of the pyrolytic products. As a result, an autothermal regime is achieved, which allows energy integration, reduces operating costs, and improves process feasibility. Furthermore, the conical spouted bed reactor avoids the hot spots created by nonhomogeneous combustion in the bed, thanks to the cyclic movement of the solid (which is assumed to be in perfect mix and without stagnation), which contributes to high heat transfer rates and allows bed isothermicity.<sup>30,31</sup>

Concerning the pyrolysis products, there are certain differences when operating under an autothermal regime. In a previous paper<sup>37</sup> on the kinetic study of the oxidative pyrolysis of pinewood, the process was described as the contribution of the following: (i) thermal pyrolysis and heterogeneous oxidation occurring over comparable time scales and (ii) char combustion. Therefore, pyrolysis mechanisms will change, with an expected increase in the gaseous fraction and water and a decrease in the yield of organic compounds in the bio-oil and char, which are due to the combustion reactions.<sup>38</sup> Bio-oil composition will also change due to the modification of pyrolysis mechanisms under an oxidative atmosphere. Moreover, oxygen activates the char and so

improves its structural characteristics; that is, a solid with a higher surface area is obtained.<sup>39</sup>

## 2. EXPERIMENTAL SECTION

**2.1. Raw Material.** The biomass used in this study is forest pinewood waste (*Pinus insignis*), which has been crushed and ground to a particle size in the 1–2 mm range and dried to a moisture content below 10 wt %. Ultimate and proximate analyses have been carried out in a LECO CHNS-932 elemental analyzer and in a TGA Q500IR thermogravimetric analyzer, respectively. The higher heating value (HHV) has been measured in a Parr 1356 isoperibolic bomb calorimeter. The main characteristics of the raw biomass are summarized in Table 1.

**Table 1. Biomass Characterization**

ultimate analysis (wt %)	
carbon	49.33
hydrogen	6.06
nitrogen	0.04
oxygen	44.57
proximate analysis (wt %)	
volatile matter	73.4
fixed carbon	16.7
ash	0.5
moisture	9.4
HHV (MJ kg <sup>-1</sup> )	19.8

**2.2. Pyrolysis Plant and Experimental Procedure.** Figure 1 shows the bench-scale plant used for the continuous pyrolysis

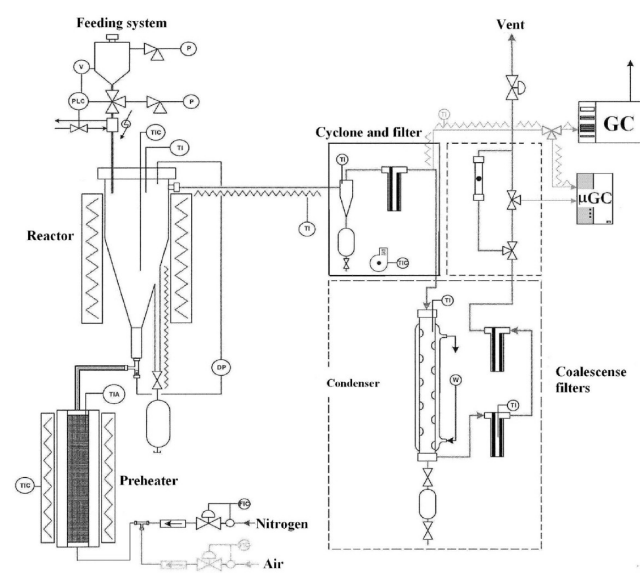


**Figure 1.** Schematic diagram of the pyrolysis pilot plant.

reactions. This unit has been set up and fine-tuned on the basis of the hydrodynamic studies carried out in a cold unit<sup>40,41</sup> and at pyrolysis reaction temperatures<sup>42</sup> and of the experience acquired in the pyrolysis of other types of wastes, such as tires,<sup>43,44</sup> plastic wastes,<sup>45,46</sup> and biomass.<sup>26,27,35</sup>

The feeding system allows the continuous feeding of the biomass and can feed up to 200 g h<sup>-1</sup> of sawdust. The nitrogen flow rate is controlled by a mass flow meter that permits feeding up to 30 L min<sup>-1</sup> and is heated to the reaction temperature by means of a preheater.

The conical spouted bed reactor consists of a lower conical section and an upper cylindrical section. Its total height is 34 cm; the height of the conical section is 20.5 cm; the angle of the conical section is 28°;

the diameter of the cylindrical section is 12.3 cm; the bottom diameter is 2 cm; and the gas inlet diameter is 1 cm. The CSBR allows continuous operation by selectively removing the char from the bed, which avoids its accumulation throughout the pyrolysis process. The fountain region of the CSBR is characterized by the segregation of different density materials, where the solids of lower density (char) describe higher trajectories, circulating near the reactor wall and allowing the removal of the char through a lateral pipe.<sup>28</sup> Further information on the reactor can be found elsewhere.<sup>35,44</sup>

The volatile products leave the reactor together with the inert gas and pass through a high-efficiency cyclone followed by a 25 mm sintered steel filter, both placed in a hot box maintained at 280 °C to prevent the condensation of heavy compounds. The vapor residence time within the fine-particle retention system is less than 1 s, avoiding the partial cracking of the vapors before their condensation. The gases leaving this filter circulate through a volatile condensation system consisting of a condenser and two coalescence filters. The condenser is a double-shell tube cooled by tap water, and the coalescence filters ensure the condensation of the aerosols remaining in the gas stream. Accordingly, the liquid collected in the condenser is mostly the aqueous phase of the bio-oil, whereas the heavier compounds that make up the organic phase are retained in the coalescence filters.

Pyrolysis runs have been conducted in autothermal mode at 500 °C (temperature at which bio-oil production is maximized)<sup>27</sup> and in continuous mode by feeding 2 g min<sup>-1</sup> of pinewood sawdust. To study the effect of oxygen on products yields and characteristics, runs have been carried out by feeding different oxygen concentrations, corresponding to 15 and 25% of the stoichiometric oxygen for complete biomass combustion. The bed was made up of 100 g of sand (particle size 0.3–0.63 mm), guaranteeing high heat transfer and bed isothermicity, and the fluidizing gas (nitrogen and air) flow rate was 1.2 times the minimum spouting velocity to ensure stable spouting.

To attain an autothermal regime in the bench-scale plant, preliminary runs have been carried out to find the protocol to follow during the start-up period. Thus, the reactor temperature at the beginning of the runs has been set to 480 °C, and the heater has been disconnected. Biomass has then been continuously fed, and temperature steadily rose to 500 °C, which is the value kept constant until the end of the run; that is, steady state was reached at this temperature. It should be pointed out that the reactor temperature has to be higher than 470 °C to ensure combustion reactions take place. Reaction temperature has also been controlled by adjusting the inlet gas temperature, which has been set to 500 °C at the beginning of the run until particle ignition occurs and, subsequently, reduced to 470 °C when 15% stoichiometric oxygen was in the feed and to 420 °C when 25% was the case.

**2.3. Product Analysis.** Product analysis has been carried out online by analyzing the reactor outlet stream with a gas chromatograph (GC) (Varian 3900) equipped with a flame ionization detector (FID). To avoid the condensation of heavy oxygenated compounds, the line from the reactor outlet to the chromatograph is heated to a temperature of 280 °C and, in addition, the reactor outlet stream has been diluted with an inert gas. A calibration has been performed to obtain the FID device's response factors to oxygenated compounds. Note that, unlike hydrocarbons, the FID response to oxygenated compounds is not proportional to their mass. Furthermore, noncondensable products leaving the condensation system have been monitored using a micro-chromatograph (Varian 4900). This micro-GC has also been used to measure the water yield, following a similar procedure to that described for the standard gas chromatograph.

In each run, 100 g of biomass have been continuously fed and samples have been taken after operating for at least 10 min under the same conditions. Each run has been repeated several times to ensure process reproducibility. The experimental error is low for most of the compounds, around 1%; however, certain products record higher uncertainty, with the error being lower than 5% in these cases. The mass balance is closed using the information obtained by weighing the char collected by the lateral outlet and at the cyclone and reactor at the end of the continuous run, and by the online chromatographic analysis. To validate the mass balance, an internal standard (cyclohexane) has been introduced in some of the experiments

through an inlet located in the heated line running from the reactor to the chromatograph, which allowed obtaining 94% mass balance closure. A more detailed description of the procedure can be found elsewhere.<sup>46</sup>

The identification of the liquid products has been performed in a GC/MS (Shimadzu UP-2010S) and the gaseous products have also been analyzed by means of a micro-GC connected to a mass spectrometer (Agilent 5975B). The fuel properties of the bio-oil have been measured by carrying out an ultimate analysis and measuring the calorific value and water content (ASTM D95 standard). The surface area and pore volume of the char have been determined from nitrogen adsorption–desorption isotherms obtained in a Micromeritics ASAP 2000. The surface characteristics of the chars have been analyzed using a JEOL JSM-6400 scanning electron microscope.

### 3. RESULTS

**3.1. Energy Estimation for the Scale-up of the Autothermal Pyrolysis Process.** The energy required for the pyrolysis process in a conical spouted bed reactor at 500 °C (temperature at which bio-oil yield is maximized),<sup>27</sup> considering two different heat recovery options, has been estimated to determine the optimum operating conditions to achieve autothermal operation. In addition, with a view to analyzing the viability of the pyrolysis process scale-up, the study has been applied to three different scales: a 200 g h<sup>-1</sup> bench-scale plant used here to carry out the pyrolysis runs, a 25 kg h<sup>-1</sup> plant located at the Ikerlan Research Centre,<sup>31</sup> and a 500 kg h<sup>-1</sup> industrial-scale plant (not yet operative). The reactor configuration is shown in Figure 2, and the geometric factors

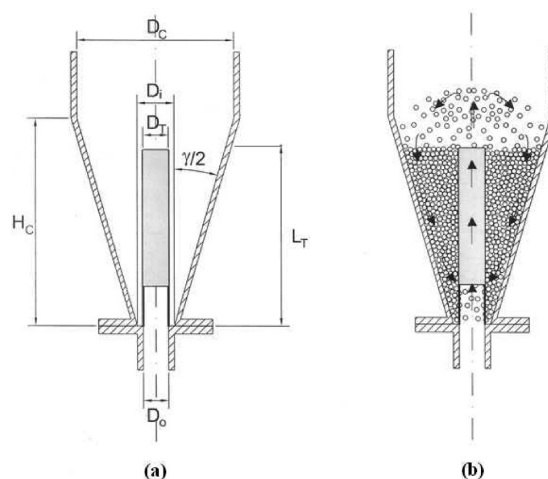


**Figure 2.** Geometric factors (a) and solid trajectories (b) in a conical spouted bed reactor with draft tube.

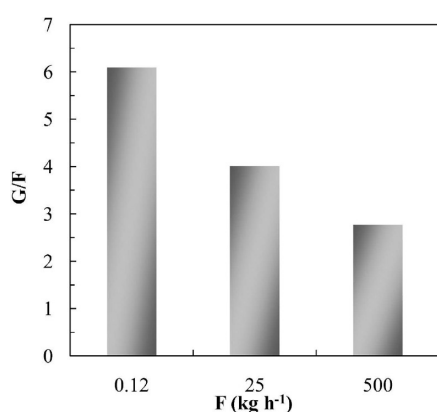
and operating conditions (at 500 °C) are summarized in Table 2. The pilot plant and industrial-scale plant are fitted with an internal device, which is a nonporous draft tube designed to improve bed stability.<sup>34</sup>

One of the most important parameters in the pyrolysis process in a spouted bed is the fluidizing gas flow rate, as its heating is one of the main energy inputs and affects the efficiency of the condensation of the volatile products. As observed in Figure 3, when the biomass feed rate ( $F$ ) is increased, the ratio between the fluidizing gas mass flow rate and biomass mass flow rate ( $G/F$ ) decreases. Thus, for a 500 kg h<sup>-1</sup> industrial plant, this value is half that for a bench-scale plant. This is one of the advantages when scaling up the conical spouted bed reactor; that is, when the biomass feed-rate is



**Table 2. Operating Parameters (at 500 °C) and Reactor Dimensions for the Pyrolysis Plants Studied**

parameters	bench-scale	pilot plant	industrial-scale
$F_{\text{biomass}}$ (kg h <sup>-1</sup> )	0.12	25	500
$Q_{\text{gas}}$ (NL min <sup>-1</sup> )	10.5	1438	19 900
$m_{\text{sand}}$ (kg)	0.1	6	250
$d_{\text{p,sand}}$ (mm)	0.3–0.63	1.05	1.4
Dimensions			
$H_T$ (cm)	34	103	283
$H_C$ (cm)	20.05	33	103
$\gamma$ (deg)	28	32.2	32
$D_C$ (cm)	12.3	24.2	90
$D_i$ (cm)	2	6.2	15.5
$D_0$ (cm)	1	4	10
$D_T$ (cm)		4	10
$L_T$ (cm)		28	95

**Figure 3.** Gas (G) and biomass (F) mass flow rates ratio for the three scales studied.

increased, the mass of inert material in the bed (sand in this case) increases proportionally, but the mass flow rate of inlet gas required for spouting the bed increases less than proportionally. The explanation for this trend lies, on the one hand, in the use of internal devices that reduce the gas flow rate required and, on the other, in a feature of the CSBR itself, whereby the conical bed is partially supported by the contactor wall. Furthermore, the conical spouted bed reactor has an additional advantage over fluidized beds given that the latter require a much higher inert solid/biomass ratio in the bed.

Consequently, these features of the CSBR mean a reduction in energy requirements for large-scale operation, thereby improving the viability of the biomass pyrolysis process. Moreover, this reduction in the rising trend of the spouting gas flow rate with bed mass alleviates some of the problems of the process, such as gas heating and bio-oil condensation.

This study has been carried out considering that the energy supplied by the combustion meets the requirements for heating the biomass and fluidizing gas to the reaction temperature and those for the pyrolysis reaction and energy losses. Therefore, the energy balance is

$$\left( \begin{array}{c} \text{combustion} \\ \text{heat} \end{array} \right) = \left( \begin{array}{c} \text{energy to heat} \\ \text{the biomass} \end{array} \right) + \left( \begin{array}{c} \text{energy to heat} \\ \text{the fluidizing gas} \end{array} \right) + \left( \begin{array}{c} \text{energy for} \\ \text{pyrolysis} \end{array} \right) + \left( \begin{array}{c} \text{energy} \\ \text{losses} \end{array} \right) \quad (1)$$

In this study, combustion heat has been assumed to be supplied only by the combustion of the raw biomass. Accordingly, the first term in eq 1 is defined as

$$\text{combustion heat} = F \times \text{ER} \times \text{HHV}_{\text{biomass}} \quad (2)$$

where ER is the equivalence ratio:

$$\text{ER} = \frac{\text{oxygen flow rate}}{\text{stoichiometric oxygen flow rate}} \times 100 \quad (3)$$

The energy required to heat the biomass to the reaction temperature has been determined by assuming that the biomass has a 10% moisture content:

$$\begin{aligned} \text{energy to heat the biomass} \\ = F C_p^{\text{biomass}} \Delta T_1 + 0.9 F C_p^{\text{biomass}} \Delta T_2 + 0.1 F \lambda_v \end{aligned} \quad (4)$$

where  $\Delta T_1$  is the difference between the ambient temperature and 100 °C and  $\Delta T_2$  between 100 °C and the reaction temperature (500 °C). The heat capacity of the biomass has been calculated using the equation proposed by Koufopoulos et al.:<sup>47</sup>

$$\begin{aligned} C_p^{\text{biomass}} &= 1.112 + (4.85 \times 10^{-3})(T - 273) \\ &(\text{kJ}(\text{kg K})^{-1}) \end{aligned} \quad (5)$$

To improve the energy efficiency of the process, the operation in an industrial pyrolysis process should be carried out by recirculating the stream of noncondensable pyrolysis gases and using it as fluidizing agent. This recirculation is carried out by condensing the volatile stream, recirculating the main fraction of the gases, and purging a small fraction for burning before it is vented. Therefore, the fluidizing gas is composed of mainly the air used to achieve the autothermal operation, apart from N<sub>2</sub>, CO, CO<sub>2</sub>, and a small amount of methane and other light hydrocarbons.<sup>27</sup> The energy required to heat the fluidizing gas is

$$\begin{aligned} \text{energy to heat the fluidizing gas} \\ = G \sum_{i=1}^i (x_i C_{p,i}) \Delta T \end{aligned} \quad (6)$$

where  $x_i$  is the molar fraction of each compound in the gaseous fraction and  $C_{p,i}$  the corresponding specific heat.

Furthermore, to improve the energy efficiency of the process, energy integration has been considered; that is, the energy required to heat the fluidizing gas is partially supplied by the volatiles that leave the reactor. These volatile products are cooled to 300 °C, which is a sufficiently high temperature to avoid condensation in the heat exchanger. The temperature of the fluidizing gas at the outlet of the heat exchanger has been determined by the commercial simulator PROII, using the product distribution obtained in a previous paper,<sup>27</sup> where pinewood pyrolysis under inert atmosphere has been studied. The temperatures calculated for the outlet gas stream are 288, 330, and 385 °C for the bench-scale plant, pilot plant, and industrial plant, respectively. Note that the higher temperature attained at a larger scale is explained by the lower G/F ratio (Figure 3).

The determination of the energy required for the biomass pyrolysis reaction has been extensively studied in the literature, and a wide range of different values have been reported.

Furthermore, from an engineering point of view, this reaction heat is often considered to be negligible compared to the other energy contributions.<sup>36</sup> The value proposed by Koufopoulos et al.<sup>47</sup> has been used here:  $-255 \text{ kJ kg}^{-1}$ . The energy losses have been assumed to be 10% of the energy supplied.

The values of the equivalence ratio (ER) required to operate under autothermal conditions have been determined for each scale studied. The results for the two options studied (with and without heat recovery of the volatiles that leave the reactor) are shown in Figure 4.

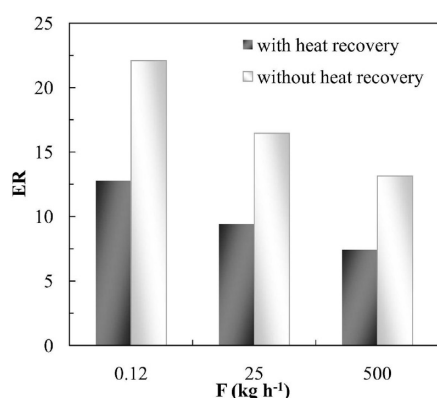


**Figure 4.** Equivalence ratios required for autothermal operation with and without energy recovery.

The equivalence ratio required to operate under autothermal conditions decreases as the process scale is larger, mainly due to the attenuation in the increase of the gas mass flow rate required at larger scale. In the option without energy recovery, the value of the equivalence ratio decreases from 22 at bench-scale plant to 13 at industrial-scale, which corresponds to 4.8 vol % oxygen in the gas stream. When the heat exchange between the volatile products leaving the reactor and the fluidizing gas is considered, there is a significant decrease in the amount of energy required, and consequently, the oxygen amount required is significantly reduced, almost by 50%. In this case, the values of the equivalence ratio range from 12.7 for the bench-scale plant to 7.3 for the industrial one. In the latter case, the oxygen concentration in the gas stream is 2.7 vol %, and consequently, the yields of pyrolysis products will not change significantly compared to those recorded in the process under inert atmosphere conditions.

Figure 5 shows a schematic diagram of the pyrolysis process at industrial-scale and with heat recovery.

**3.2. Continuous Oxidative Flash Pyrolysis in the Bench-Scale Conical Spouted Bed Unit.** Based on the information obtained in the energy study, oxidative pyrolysis runs have been carried out using pinewood in the bench-scale plant at  $500^\circ\text{C}$ , with equivalence ratios of 15 and 25, and the results have been compared with those obtained in pyrolysis with an inert atmosphere. As mentioned in the Experimental Section, the runs performed with the two equivalence ratios have been carried out under autothermal conditions, which allows assessing the effect of oxygen concentration on products yields and properties under these conditions. The oxygen concentrations in the fluidizing gas stream are 2.5 and 4.1 vol % for the equivalence ratios of 15 and 25, respectively. This information is essential for the autothermal oxidative pyrolysis

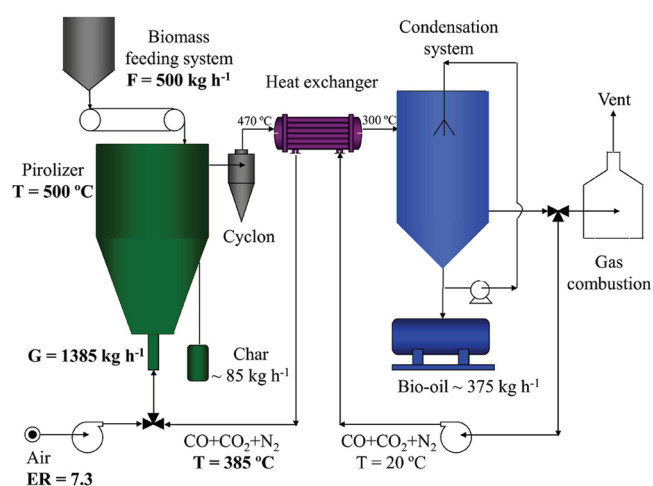


**Figure 5.** Schematic diagram of the autothermal operation at industrial scale with heat recovery.

process at a large scale, given that oxygen inlet concentration is the operating variable to be controlled.

**3.2.1. Product Yields.** The products have been grouped into three different fractions: gas fraction, bio-oil, and char. The product yields have been defined by mass unit of the biomass in the feed (g/100 g biomass) to make easier the comparison of the results with those obtained without oxygen addition. It should be noted that the oxygen introduced in the fluidizing gas is also a reactant in the pyrolysis process, and consequently, the sum of the yields of the fractions is higher than 100. The influence of oxygen addition on product yields is shown in Table 3, where the results are given by mass unit of raw biomass.

**Table 3. Effect of Oxygen on the Yields of the Different Product Fractions at  $500^\circ\text{C}$  (g/100 g biomass)**

fraction	ER		
	0	15	25
gas	7.3	21.4	30.7
bio-oil	75.3	84.3	90.2
water	25.4	36.0	43.2
char	17.3	12.9	10.1
total	100.0	118.6	131.0

As expected, when oxygen is added to the reaction environment, gas and water yields increase, whereas char yield decreases.

The gas yield increases considerably as a result of the formation of combustion products, mainly carbon dioxide. When 15% of the stoichiometric oxygen is added, which accounts for 2.5 vol % oxygen in the gas stream, the gas yield obtained is three times that in inert pyrolysis, and 30.7 g/100 g biomass is obtained when an ER of 25 is used.

Bio-oil yield increases when oxygen is added, up to 90.2 g/100 g biomass for an equivalence ratio of 25 (4.1 vol % oxygen in the fluidizing gas stream). This increase is due to the rise in water yield by partial combustion reactions. However, the yield of organic compounds in the bio-oil is approximately the same, around 50 g/100 g biomass, or slightly lower in the oxidative process. As reported in previous papers,<sup>27,35</sup> the bio-oil yield in the conical spouted bed reactor is very high as a result of this reactor's suitable features for the maximization of the liquid yield, namely, high heat and mass transfer rates, low volatile residence time, and continuous removal of char from the bed.<sup>5</sup>

Finally, char yield decreases from 17.3 to 10.1 g per 100 g of biomass when operating with an equivalence ratio of 25. The char is not completely burned because of the lack of oxygen in the reaction environment and because it is rapidly removed from the reactor through the lateral pipe.

Considering these results, it can be concluded that the energy required for the pyrolysis process is obtained mainly by char combustion and, to a lesser extent, by the combustion of the gas fraction (carbon monoxide and  $C_1$ – $C_4$  hydrocarbons) and a small part of the condensable fraction (bio-oil). These results are a direct consequence of the residence time of both the volatiles and the char in the reaction environment; that is, the volatile stream leaves the reactor in less than 1 s, whereas the char on average needs around 2 min.

The most similar paper published on biomass autothermal pyrolysis is that by Boukis et al.,<sup>38</sup> who performed pinewood pyrolysis in a circulating fluidized bed reactor, where autothermal regime is obtained by separating and recirculating the char fraction for its combustion in a separate bed. Operating at 500–600 °C with pinewood sawdust and equivalence ratios in the 20–30 range, they obtained a maximum liquid amount of 70 g/100 g biomass at 500 °C and for ER = 22.6.

Furthermore, Suarez et al.<sup>48</sup> also carried out pinewood autothermal pyrolysis in a fluidized bed, except operating at higher temperatures, around 675–800 °C, and they obtained mainly gaseous products. Finally, Scott et al.<sup>49</sup> patented a process to maximize levoglucosan production, subjecting the biomass first to a deionization treatment and, subsequently, to a fast pyrolysis process under conditions of controlled oxidation to remove lignin-derived products. Nevertheless, when they carried out oxidative pyrolysis without subjecting the biomass to the deionization process at 450–490 °C, 68 g of gas, 32.2 g of organic fraction, 27.5 g of water, and 12.7 g of char were obtained from 100 g of biomass.

**3.2.2. Gas Fraction.** The gas fraction is mainly made up of carbon dioxide and carbon monoxide, and as shown in Table 4, their yields increase when oxygen is added.

**Table 4. Influence of the Equivalence Ratio on Gaseous Product Yields (g/100g biomass)**

cmpd	ER		
	0	15	25
carbon dioxide	3.27	15.64	24.01
carbon monoxide	3.38	5.14	6.21
hydrogen	0.004	0.00	0.00
methane	0.36	0.34	0.21
ethylene	0.09	0.09	0.13
ethane	0.06	0.04	0.04
propylene	0.07	0.09	0.07
propane	0.05	0.02	0.01
2-methyl-1-propene	0.02	0.03	0.03
2-butene	0.01	0.02	0.02
unidentified	0.01	0.00	0.00
gas	7.33	21.40	30.74

The yield of carbon dioxide increases significantly with the equivalence ratio, but the CO increase is less pronounced. The methane amount decreases, and that of  $C_2$ – $C_4$  hydrocarbons remains almost constant. However, the alkene yield increases slightly, probably as a result of radical formation when oxygen is added to the reaction.<sup>50</sup> Similar trends have been observed by other authors.<sup>38,48</sup>

Furthermore, when these results are expressed in terms of concentration (Figure 6), it is observed that the concentration

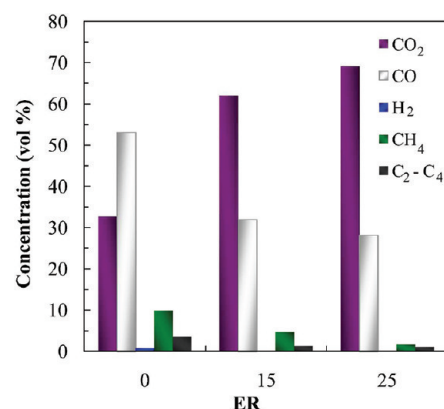


**Figure 6. Influence of oxygen addition on gas composition.**

of all the compounds except  $CO_2$  decreases when the equivalence ratio is increased, which is due to the combustion reactions. When 25% of the stoichiometric oxygen is fed, carbon dioxide accounts for almost 70 vol % of the gas fraction. However, because oxygen concentration is below the stoichiometric value, there is still a significant amount of CO and  $C_1$ – $C_4$  hydrocarbons, although their concentrations are significantly lower than those for lower equivalence ratios. Therefore, as the amount of oxygen fed into the reactor is increased, the calorific value of the gas decreases, which is evidence that the gas fraction has contributed to supplying the energy required to ensure autothermal operation.

**3.2.3. Bio-oil Composition and Properties.** Bio-oil is a very complex mixture of oxygenated compounds, so, in order to simplify the results, the products have been lumped according to their functional groups. Table 5 shows the yields of the functional groups and certain main products. More than 110 compounds have been identified with high quality, accounting for more than 83 wt % of the whole bio-oil.

The main compound in the liquid fraction is water, and its yield increases considerably by adding oxygen in the feed, as a result of combustion reactions. Water is formed from the moisture in the biomass, from the dehydration of cellulose and hemicellulose, and from the combustion of gas and char. The water amount increases by 70% when 25% of the stoichiometric oxygen is added, reaching a value of 43 g/100 g biomass.

Concerning the organic compounds, the yield of total organic oxygenates undergoes only a slight reduction when operating under oxidative conditions. The yields obtained a range from 49.97 g/100 g biomass for the pyrolysis under an inert atmosphere to 46.93 g/100 g biomass for the autothermal pyrolysis with 4.1 vol % oxygen. Furthermore, the products identified in the oxidative pyrolysis are almost the same as those in inert pyrolysis.

Bio-oil is composed mainly of phenols, whose yield passes through a minimum for an equivalence ratio of 15. This is an interesting result for the upgrading of bio-oil by catalytic reforming, given that phenols are catalyst-resistant and contribute to the deposition of pyrolytic lignin on the catalyst.<sup>51</sup> This group has, in turn, been divided into three other lumps: guaiacols (methoxyphenols), catechols (benzenediols), and alkyl-phenols. As shown in Table 5, guaiacols are the main phenolic products and their yield passes through a minimum at ER = 15 and then increases as oxygen concentration is

**Table 5. Effect of Oxygen Concentration on the Yields (g/100 g biomass) of the Functional Groups and Main Individual Components in the Bio-oils Obtained in Inert and Oxidative Pyrolysis**

cmpd	ER		
	0	15	25
acids	2.73	3.72	3.84
formic acid	0.17	0.31	0.28
acetic acid	1.11	0.54	0.67
propanoic acid	0.14	0.40	0.29
dimethylbenzoic acids	0.26	0.38	0.62
alcohols	2.00	2.07	1.86
methanol	0.69	0.47	0.49
glycerin	1.11	1.36	1.09
aldehydes	1.93	2.21	1.70
formaldehyde	0.35	0.82	0.72
acetaldehyde	0.16	0.15	0.13
2-propenal	0.12	0.05	0.05
benzaldehydes	0.49	0.55	0.24
furans	3.32	3.46	2.89
furan	0.71	0.42	0.20
2-furanmethanol	0.75	1.27	1.16
tetrahydro 2-furanmethanol	1.17	0.38	0.09
ketones	6.44	7.52	6.37
acetone	0.67	0.02	0.02
acetol	1.53	1.37	0.92
cyclopentanediones	0.52	0.98	0.89
cyclohexanone	1.23	0.95	0.68
hydroxymethoxyphenyl ketones	1.09	1.51	1.60
phenols	16.49	13.45	15.31
alkyl phenols	1.80	2.16	2.21
phenol	0.40	0.26	0.26
cresols	0.67	1.40	1.34
catechols	7.16	4.50	3.93
catechol	4.08	2.25	1.60
methyl catechols	2.40	1.05	0.98
guaiacols	7.48	6.65	9.04
guaiacol	1.86	0.58	1.21
eugenol	1.40	2.04	2.79
saccharides	4.46	0.37	0.35
2,3-anhydro-d-mannosan	1.56	0.00	0.00
levoglucosan	2.78	0.37	0.35
others	0.06	0.74	0.78
unidentified	12.61	16.35	15.13
total organic oxygenates	49.97	48.33	46.93
water	25.36	35.97	43.22
bio-oil	75.33	84.30	90.15

increased. This rise is caused by the increase in guaiacol, 4-vinyl guaiacol, and eugenol yields. However, the catechol yield decreases as the equivalence ratio is increased, being half that obtained in inert pyrolysis when the equivalence ratio is 25. Finally, alkyl phenols increase slightly when oxygen is added to the pyrolysis reaction, probably as a result of the increase in temperature inside the biomass particle, which leads to an intensification of secondary recombination and cyclization reactions.<sup>52</sup>

Ketones are one of the prevailing functional groups, and as observed in Table 5, their yield peaks at an equivalence ratio of 15. Heavy ketones contribute to this increase, but the yield of the light ones (acetone and acetol) decreases when oxygen is added, presumably as a result of combustion reactions.

Saccharides make up a significant lump in thermal pyrolysis, but their yield decreases dramatically when oxygen is introduced. Scott et al.<sup>49</sup> observed a similar trend, with a low levoglucosan yield, which was lower in the oxidative pyrolysis than in the inert one.

Concerning furans, their yield peaks at an equivalence ratio of 15, but decreases when 25% of the stoichiometric oxygen is introduced, as a result of the reduction in the yields of furan and 2-tetrahydrofuranmethanol. The acid group is the only one that increases with equivalence ratio, although acetic yield decreases.

With regard to alcohols, the yield of this group remains almost constant, and methanol yield decreases, whereas glycerin passes through a smooth maximum. Finally, the yield of aldehydes does not change significantly.

It can therefore be concluded that the compound that is mostly affected by oxygen addition is water, whose yield increases considerably. However, the total yield of organic oxygenates does not change significantly when operating with up to 4.1 vol % oxygen. Regarding individual compounds, guaiacols, catechols, and saccharides are the ones most influenced by oxygen addition, whereas the yields of the remaining compounds do not undergo significant changes.

**Table 6. Effect of Oxygen Addition on Bio-oil Properties**

properties	ER		
	0	15	25
water content (wt %)	36.7	44.9	50.3
HHV (MJ kg <sup>-1</sup> )	14.6	11.9	9.5
Ultimate Analysis (wt %)			
carbon	41.7	37.6	33.3
hydrogen	8.1	8.4	8.8
nitrogen	0.2	0.3	0.3
oxygen	50.0	53.6	57.6

Furthermore, the bio-oil has been characterized by carrying out an ultimate analysis and measuring its water content and calorific value. The results are shown in Table 6.

Because of the high amount of water formed by combustion reactions, the liquid obtained in the oxidative pyrolysis is more oxygenated than that obtained in inert pyrolysis, and carbon content decreases when the equivalence ratio is increased. Water content is very high, and with an equivalence ratio of 25,

**Table 7. Effect of Oxygen Addition on Char Properties**

properties	ER		
	0	15	25
Ultimate Analysis (wt %)			
carbon	82.7	75.8	72.5
hydrogen	2.9	3.0	2.9
nitrogen	0.1	0.0	0.2
oxygen	11.4	17.3	19.5
Proximate Analysis (wt %)			
volatile matter	23.5	24.9	27.2
fixed carbon	73.6	71.2	67.8
ash	2.9	3.9	5
HHV (MJ kg <sup>-1</sup> )	30.4	23.2	20.9
Surface Characteristics			
BET surf. (m <sup>2</sup> g <sup>-1</sup> )	16.2	23.6	8.1
avg pore diam. (Å)	389.7	341.4	422.0



it accounts for almost half the liquid fraction. Consequently, the calorific value of the liquid is very low and decreases as the oxygen amount introduced into the reactor is higher. Other bio-oil properties, such as pH, density, viscosity, and stability

will also be influenced by the high water content, which requires subsequent studies.

Therefore, the conical spouted bed reactor is a suitable technology for oxidative pyrolysis, given that the oxygen content required to attain an autothermal regime decreases when the scale is increased and product properties are not significantly affected.

**3.2.4. Char Characterization.** The char particles keep the original shape of the sawdust particles, but they are more fragile and porous, and have higher carbon content. On the basis of these properties, char is suitable for providing energy to the process, or it may also be used as active carbon (after being subjected to an activation process) or as a soil amender.<sup>13–16</sup> The char has been characterized by ultimate and proximate analyses, calorific value quantification, and surface and structural property measurement (Table 7).

The ultimate and proximate analyses confirm that part of the char is burned during the oxidative pyrolysis and this heat contributes to supplying energy to the reaction. Carbon and fixed carbon contents are reduced when the equivalence ratio is increased. However, even when operating with 25% of the stoichiometric oxygen amount, carbon content in the char is 72.5 wt % and the ash content is merely 5 wt %, which is evidence that the char has only partially combusted, as previously commented. Therefore, the calorific value of the char decreases when oxygen is incorporated into the reaction environment.

Regarding structural properties, the chars obtained in these reactions have very low BET areas, and the pores formed are macropores and mesopores. However, the addition of a small amount of oxygen has a positive effect on surface properties, given that the surface area increases from  $16.2 \text{ m}^2 \text{ g}^{-1}$  without oxygen to  $23.6 \text{ m}^2 \text{ g}^{-1}$  with an equivalence ratio of 15, and furthermore, narrower pores are also formed.

These results are attributable to the lower combustion rate inside the biomass particle for lower oxygen concentrations in the reaction environment, which leads to a more homogeneous porosity development. Conversely, when the oxygen concentration is higher, the char combustion rate is higher, generating macropores and high mass loss values. This aspect has already been observed in air activation studies,<sup>53,54</sup> in which an accurate control of oxygen concentration is the key factor to avoid uncontrolled combustion and, consequently, to optimize the porous structure, especially the formation of micropores and mesopores.<sup>39,55</sup>

The porous surface structure of the solids has been characterized by means of scanning electron microscopy (SEM) analysis, Figure 7. It is observed that the char obtained in inert pyrolysis has a smoother surface with vaguely defined grooves, whereas the char obtained with an equivalence ratio of 15 has a rougher surface with clearly defined grooves. The char obtained operating with 25% of the stoichiometric oxygen has a more irregular surface and fewer grooves than the char obtained in inert pyrolysis.

#### 4. CONCLUSION

Autothermal operation can be achieved in the oxidative flash pyrolysis of biomass in a conical spouted bed reactor. This reactor has proven to be a suitable technology for scaling up the pyrolysis process. Thus, the gas flow rate required for stable spouting does not increase proportionally to the mass in the bed, and consequently, the oxygen concentration that has to be added for the process to operate autothermally is also lower,

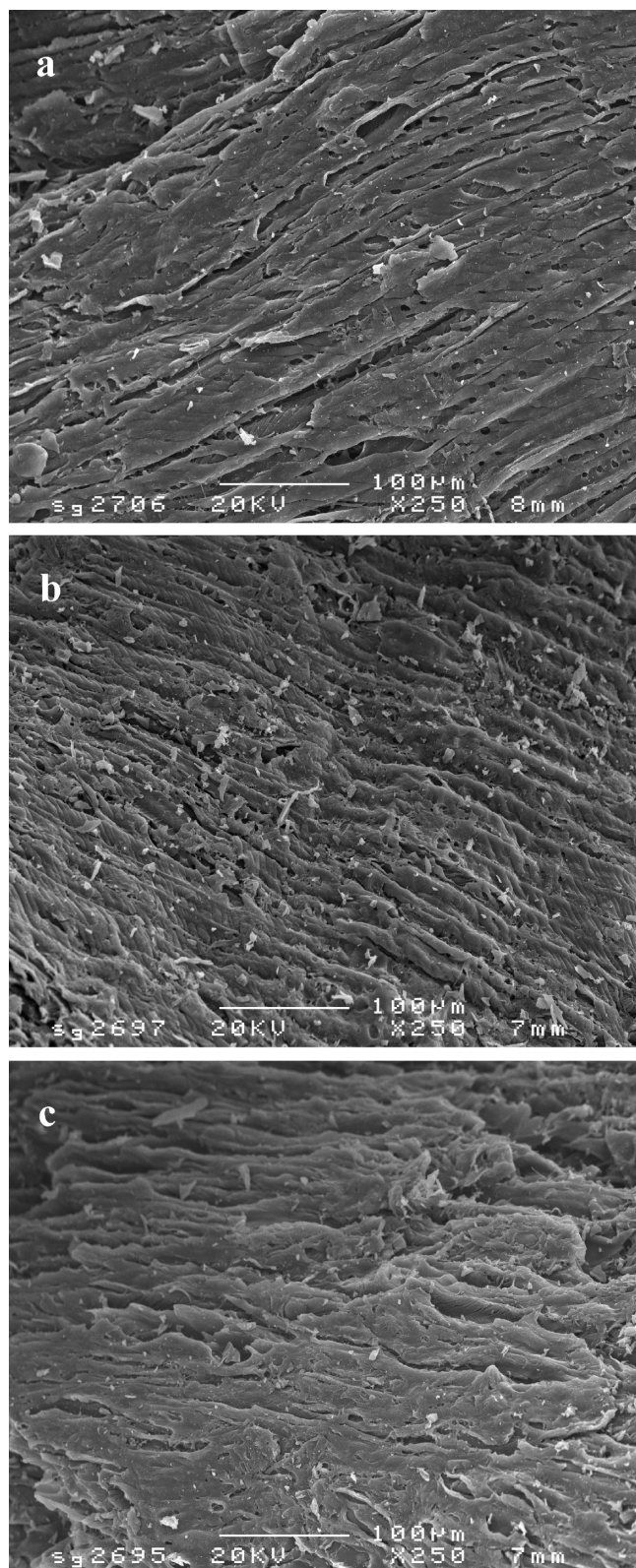


**Figure 7.** SEM photomicrographs of chars obtained at 500 °C in inert (a) and oxidative pyrolysis with equivalence ratios of 15 (b) and 25 (c).

restricting the influence of secondary combustion reactions in the pyrolysis products. Thus, at an industrial scale (500 kg h<sup>-1</sup>) and with energy recovery (heat exchange between the volatiles leaving the reactor and the fluidizing gas), only 2.7 vol % oxygen in the gas stream is required to operate under autothermal conditions.

In the bench-scale study at 500 °C and adding up to 4.1 vol % oxygen in the gas stream (25% of the stoichiometric oxygen), it has been observed that the gas yield increases significantly, mainly as a result of the formation of carbon dioxide. The bio-oil yield increases from 75.3 to 90.2 g/100 g biomass in the oxygen concentration range studied, although this increase is due to the higher water yield. Nevertheless, the yield of organic oxygenated compounds decreases only from 49.9 to 46.9 g/100 g biomass. Char yield decreases in oxidative pyrolysis; that is, it is not completely burned because of the lack of oxygen and its continuous removal from the reaction environment. Consequently, it keeps a high calorific value and its surface properties are slightly improved. Accordingly, the energy required for the pyrolysis process is obtained mainly by char combustion and, to a lesser extent, by the combustion of the gas phase (carbon monoxide and C<sub>1</sub>–C<sub>4</sub> hydrocarbons) and a small part of the bio-oil.

Bio-oil composition is influenced slightly by adding up to 4.1 vol % oxygen to the inlet gas stream, with water being the most affected compound and, to a lesser extent, guaiacols, catechols, and saccharides. Phenol yield decreases slightly, and consequently, a more suitable bio-oil for catalytic upgrading is obtained. Bio-oil fuel properties are diminished as a result of the high water content, and therefore, low oxygen concentrations should be used. The conical spouted bed reactor allows autothermal operation at large scale (500 kg h<sup>-1</sup>) with an oxygen concentration in the spouting gas stream of only 2.7 vol %. In addition, because of the features of this technology, the oxygen concentration required for autothermal operation decreases when scaling up the process, which is essential for obtaining a high yield of bio-oil by oxidative pyrolysis without compromising quality.

## AUTHOR INFORMATION

### Corresponding Author

\*Telephone: +34946012527. Fax: +34946013500. E-mail: martin.olazar@ehu.es.

## ACKNOWLEDGMENTS

This work was carried out with the financial support of the Ministry of Science and Education of the Spanish Government (Project CTQ2010-16133) and of the Basque Government (Project GIC07/24-IT-220-07), as well as with a bursary for research training of the Basque Government (BFI06.329).

## NOMENCLATURE

- $C_p^{\text{biomass}}$ ,  $C_{p,i}$  = specific heat (kJ (kg K<sup>-1</sup>)).  
 $D_0$  = gas inlet diameter (cm).  
 $D_C$  = diameter of the conical section of the reactor (cm).  
 $D_i$  = diameter of the reactor base (cm).  
 $d_{p,\text{sand}}$  = sand particle diameter (mm).  
 $D_T$  = draft tube diameter (cm).  
 $ER$  = equivalence ratio.  
 $F$  = biomass feed rate (kg h<sup>-1</sup>).  
 $G$  = gas mass flow rate (kg h<sup>-1</sup>).  
 $H_C$  = height of the conical section of the reactor (cm).

$H_T$  = total reactor height (cm).

$L_T$  = draft tube height (cm).

$m_{\text{sand}}$  = inert bed material (sand) mass (kg).

$Q_{\text{gas}}$  = gas volumetric flow rate (NL min<sup>-1</sup>).

$x_i$  = molar fraction.

$\gamma$  = cone included angle of the reactor (deg).

$\lambda_v$  = water vaporization enthalpy (kJ kg<sup>-1</sup>).

## REFERENCES

- (1) Fernando, S.; Adhikari, S.; Chandrapal, C.; Murali, N. *Energy Fuels* **2006**, *20*, 1727–1737.
- (2) Demirbas, A. *Energy Convers. Manage.* **2009**, *50*, 2239–2249.
- (3) FitzPatrick, M.; Champagne, P.; Cunningham, M.; Whitney, R. *Bioresour. Technol.* **2010**, *101*, 8915–8922.
- (4) Czernik, S.; Bridgwater, A. *Energy Fuels* **2004**, *18*, 590–598.
- (5) Bridgwater, A. V. *Biomass Bioenergy* **2011**, DOI: 10.1016/j.biombioe.2011.01.048.
- (6) Gayubo, A. G.; Valle, B.; Aguayo, A. T.; Olazar, M.; Bilbao, J. *Ind. Eng. Chem. Res.* **2010**, *49*, 123–131.
- (7) Valle, B.; Gayubo, A. G.; Aguayo, A. T.; Olazar, M.; Bilbao, J. *Energy Fuels* **2010**, *24*, 2060–2070.
- (8) Wu, C.; Huang, Q.; Sui, M.; Yan, Y.; Wang, F. *Fuel Process. Technol.* **2008**, *89*, 1306–1316.
- (9) Corma, A.; Huber, H.; Sauvanaud, L.; O'Connor, P. *J. Catal.* **2007**, *247*, 307–327.
- (10) Gayubo, A. G.; Valle, B.; Aguayo, A. T.; Olazar, M.; Bilbao, J. *Energy Fuels* **2009**, *23*, 4129–4136.
- (11) Mohan, D.; Pittman, C.; Steele, P. *Energy Fuels* **2006**, *20*, 848–889.
- (12) Neves, D.; Thunman, H.; Matos, A.; Tarelho, L.; Gómez-Barea, A. *Prog. Energy Combust. Sci.* **2011**, *37*, 611–630.
- (13) Ioannidou, O.; Zabaniotou, A. *Renew. Sust. Energy Rev.* **2007**, *11*, 1966–2005.
- (14) Calvo, I.; Gilarranz, M. A.; Casas, J. A.; Mohedano, A. F.; Rodriguez, J. J. *Chem. Eng. J.* **2010**, *163*, 212–218.
- (15) Bedia, J.; Barrionuevo, R.; Rodriguez-Mirasol, J.; Cordero, T. *Appl. Catal., B* **2011**, *103*, 302–210.
- (16) Jha, P.; Biswas, A. K.; Lakaria, B. L.; Rao, S. A. *Curr. Sci.* **2010**, *99*, 1218–1225.
- (17) Boateng, A.; Dagaard, D.; Goldberg, N.; Hicks, K. *Ind. Eng. Chem. Res.* **2007**, *46*, 1891–1897.
- (18) Garcia-Perez, M.; Wang, X.; Shen, J.; Rhodes, M.; Tian, F.; Lee, W.; Wu, H.; Li, C. *Ind. Eng. Chem. Res.* **2008**, *47*, 1846–1854.
- (19) Heo, H. S.; Park, H. J.; Park, Y. K.; Ryu, C.; Suh, D. J.; Suh, Y. W.; Yim, J. H.; Kim, S. S. *Bioresour. Technol.* **2010**, *101*, 1–6.
- (20) Oasmaa, A.; Kuoppala, E.; Solantausta, Y. *Energy Fuels* **2003**, *17*, 433–443.
- (21) Oasmaa, A.; Solantausta, Y.; Arpiainen, V.; Kuoppala, E.; Sipilä, K. *Energy Fuels* **2010**, *24*, 1380–1388.
- (22) Tzanetakis, T.; Ashgriz, N.; James, D.; Thomson, M. *Energy Fuels* **2008**, *22*, 2725–2733.
- (23) Léde, J.; Broust, F.; Ndiaye, F. T.; Ferrer, M. *Fuel* **2007**, *86*, 1800–1810.
- (24) Ingram, L.; Mohan, D.; Bricka, M.; Steele, P.; Strobel, D.; Crocker, D.; Mitchell, B.; Mohammad, J.; Cantrell, K.; Pittman, C. *Energy Fuels* **2008**, *22*, 614–625.
- (25) Garcia-Perez, M.; Chaala, A.; Pakdel, H.; Kretschmer, D.; Roy, C. *J. Anal. Appl. Pyrolysis* **2007**, *78*, 104–116.
- (26) Aguado, R.; Olazar, M.; San Jose, M. J.; Aguirre, G.; Bilbao, J. *Ind. Eng. Chem. Res.* **2000**, *39*, 1925–1933.
- (27) Amutio, M.; Lopez, G.; Artetxe, M.; Elordi, G.; Olazar, M.; Bilbao, J. *Resour., Conserv. Recycl.* **2012**, *59*, 23–31.
- (28) Olazar, M.; San José, M. J.; Peñas, F. J.; Aguayo, A. T.; Bilbao, J. *Ind. Eng. Chem. Res.* **1993**, *32*, 2826–2834.
- (29) Artetxe, M.; Lopez, G.; Amutio, M.; Elordi, G.; Olazar, M.; Bilbao, J. *Ind. Eng. Chem. Res.* **2010**, *49*, 2064–2069.
- (30) Freiras, L. A. P.; Freire, J. Y. *Powder Technol.* **2001**, *114*, 152–162.

- (31) Makibar, J.; Fernandez-Akarregi, A. R.; Alava, I.; Cueva, F.; Lopez, G.; Olazar, M. *Chem. Eng. Process.* **2011**, *50*, 790–798.
- (32) San José, M. J.; Olazar, M.; Peñas, F. J.; Arandes, J. M.; Bilbao, J. *Chem. Eng. Sci.* **1995**, *50*, 2161–2172.
- (33) Calonaci, M.; Grana, R.; Hemings, E.; Bozzano, G.; Dente, M.; Ranzi, E. *Energy Fuels* **2010**, *24*, 5727–5734.
- (34) Altzibar, H.; Lopez, G.; Aguado, R.; Alvarez, S.; San José, M. J.; Olazar, M. *Chem. Eng. Technol.* **2009**, *32*, 463–469.
- (35) Amutio, M.; Lopez, G.; Aguado, R.; Artetxe, M.; Bilbao, J.; Olazar, M. *Energy Fuels* **2011**, *25*, 3950–3960.
- (36) Boukis, I.; Grammelis, P.; Bezerghianni, S.; Bridgwater, A. V. *Fuel* **2007**, *86*, 1372–1386.
- (37) Amutio, M.; Lopez, G.; Aguado, R.; Artetxe, M.; Bilbao, J.; Olazar, M. *Fuel* **2011**, DOI: 10.1016/j.fuel.2011.10.008.
- (38) Boukis, I.; Grammelis, P.; Bezerghianni, S.; Bridgwater, A. V. *Fuel* **2007**, *86*, 1387–1395.
- (39) Py, X.; Guillot, A.; Cagnon, B. *Carbon* **2003**, *41*, 1533–1543.
- (40) Olazar, M.; San Jose, M. J.; Aguayo, A. T.; Arandes, J. M.; Bilbao, J. *Ind. Eng. Chem. Res.* **1993**, *32*, 1245–1250.
- (41) Olazar, M.; San Jose, M. J.; Llamasas, R.; Bilbao, J. *Ind. Eng. Chem. Res.* **1994**, *33*, 993–1000.
- (42) Olazar, M.; Lopez, G.; Altzibar, H.; Aguado, R.; Bilbao, J. *Can. J. Chem. Eng.* **2009**, *87*, 541–546.
- (43) Arabiourrutia, M.; Lopez, G.; Elordi, G.; Olazar, M.; Aguado, R.; Bilbao, J. *Chem. Eng. Sci.* **2007**, *62*, 5271–5275.
- (44) Lopez, G.; Olazar, M.; Amutio, M.; Aguado, R.; Bilbao, J. *Energy Fuels* **2009**, *23*, 5423–5431.
- (45) Lopez, G.; Artetxe, M.; Amutio, M.; Elordi, G.; Aguado, R.; Olazar, M.; Bilbao, J. *Chem. Eng. Process.* **2010**, *49*, 1089–1094.
- (46) Elordi, G.; Olazar, M.; Lopez, G.; Artetxe, M.; Bilbao, J. *Ind. Eng. Chem. Res.* **2011**, *50*, 6650–6659.
- (47) Koufopoulos, C.; Papayannakos, N.; Maschio, G.; Lucchesi, A. *Can. J. Chem. Eng.* **1991**, *69*, 907–915.
- (48) Suarez, J.; Beaton, P.; Zanzi, R.; Grimm, A. *Energy Sources, Part A* **2006**, *28*, 695–704.
- (49) Scott, D. S.; Piskorz, J.; Radlein, D.; Majerski, P. United States Patent No. 5395455, 1995.
- (50) Thomas, S.; Ledesma, E.; Wornat, M. *Fuel* **2007**, *86*, 2581–2595.
- (51) Gayubo, A. G.; Valle, B.; Aguayo, A. T.; Olazar, M.; Bilbao, J. *J. Chem. Technol. Biotechnol.* **2010**, *85*, 132–144.
- (52) Demirbas, A. *Energy Convers. Manage.* **2000**, *41*, 633–646.
- (53) Dai, X.; Antal, M. J. *Eng. Chem. Res.* **1999**, *38*, 3386–3395.
- (54) Tam, M. S.; Antal, M. J. *Ind. Eng. Chem. Res.* **1999**, *38*, 4268–4276.
- (55) Heras, F.; Alonso, N.; Gilarranz, M.; Rodriguez, J. J. *Ind. Eng. Chem. Res.* **2009**, *48*, 4664–4670.